SLC – STATUS AND DEVELOPMENT*

G. E. FISCHER (FOR THE SLC STAFF)

Stanford Linear Accelerator Center
Stanford University, Stanford, California, 94305

Summary

The status of a three year construction program, begun October 1, 1983, of the SLAC Linear Collider[1,2] is reviewed and evolutions of the original conceptual design are discussed.

Subsystems of the project, that are described with emphasis on new or unusual technology, include: Electron Source and Injector, Damping Rings, Linear Accelerator Development, Energy (Klystron and Modulator) Upgrades, Positron Production and Reinjection, Arc Transport, Final Focus System, Control System and Conventional Facilities.

Results from the commissioning program, which began in early 1986, and plans for the operation of the machine are presented.

Introduction

The SLAC Linear Collider project (SLC) which was proposed in 1980 and formally begun in October 1983 is nearing completion. Commissioning of subsystems up to the end of the linac is now underway with final completion of the remaining systems estimated before the end of the calender year.

The original goals of this project remain in effect today. They are two-fold; to provide sufficient numbers of electron-positron collisions in the 100 GeV (center of mass) region with which to examine Zo physics in detail, and to provide an experimental test bed for advancing the accelerator theory and technology of linear colliders.

The SLC is not a linear collider in the truest sense, namely pointing two linacs at each other. Rather, it is an adaption of the existing SLAC facilities to which damping rings have been added near injection and transport lines have been added to the end of the accelerator to bring intense, very small phase space beams into collision.

The main performance specifications are shown in Table 1. The column labeled "First Year" shows values we hope to attain with the collider in its initial form, the column labeled "Nominal" shows our eventual goals. These differences will be commented on in the various following sections on components, however one may note that with even a luminosity of 6×10^{29} cm^{-2}sec^{-1}, Zo's are expected to be produced at a rate of 65 hadronic decays per hour.

An overall schematic drawing of the SLC is shown in Figure 1. Let us briefly trace the steps of an operating cycle beginning at a time when each of the two damping rings have circulating in them two damped bunches. Start the cycle by extracting one bunch of positrons from the south ring and 59 nanoseconds later extract both electron bunches from the north ring. Each ring to linac (RTL) transport line contains a longitudinal phase compressor which transforms the length of each bunch from its ring equilibrium value ($\sigma_z = 6$ mm) to about 1.5 mm, suitable for matching into the linac RF structure.

Table 1: Luminosity Specifications			
	First Year	Nominal	Units
Beam Energy	50	50	E (GeV)
Repetition Rate	120[a]	180	f (sec^{-1})
Interaction Flux	5×10^{10}	7.2×10^{10}	$N \pm (e^{\pm}$/bunch)
Normalized Emittance (at RTL)	3×10^{-5}	3×10^{-5}	$\gamma\epsilon$ (m rad)
Effective Emittance (at FF)	4.2×10^{-10}	4.2×10^{-10}	$\epsilon_{x,y}$ (m rad)
Momentum Spread	± 0.2	± 0.2	$\frac{\Delta P}{P}$ (percent)
Bunch Length (Linac)	1.5	1.5	σ_z (mm)
Bunch Length (IP)	1.0[b]	1.0[b]	σ_z (mm)
Final Demagnification	4[c]	5	
Spot Size (IP)	2.07	1.65	$\sigma_{x,y}$ (μm)
Disruption Parameter	0.34	0.76	D
Pinch Factor	1.14	2.2	H
LUMINOSITY	6.4×10^{29}	6.0×10^{30}	cm^{-2} sec^{-1}

(a) Assumes technical contingency exercised initially.

(b) Assumes σ_z compression in arcs due to p/z correlation.

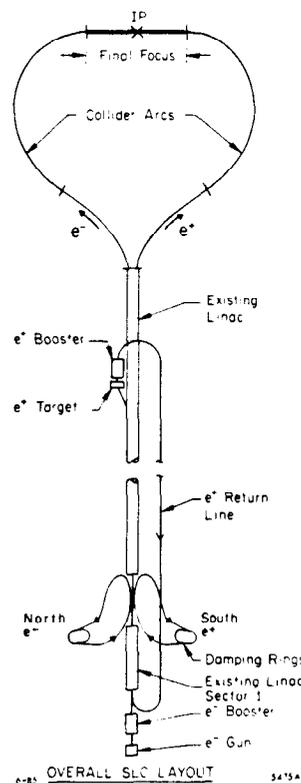(c) Assumes conventional iron quadrupoles initially.

Figure 1. Overall SLC Layout.

The first two bunches (e^+, e^-) are accelerated to the end of the linac, transported around their respective Arcs (suitably adjusted in length), demagnified to transverse dimensions of a few microns in the final focus system (FFS) and brought into collision at the interaction point (IP). Following their disruptive interaction the beams are extracted and discarded into a dump.

The third bunch, designated the scavenger bunch as it uses up some of the remaining RF in the linac, is extracted 2/3 of the way down the linac and targeted to produce positrons. These are collected and accelerated to 200 MeV in a high gradient strongly focused linac, turned around and sent down a 2 km line to the beginning of the linac for reinjection and subsequent acceleration to 1.21 GeV. Just prior to their arrival the electron gun is fired producing two bursts of particles spaced 59 nanoseconds apart which are chopped, phase compressed and also accelerated to 1.21 GeV for injection into their ring in which they are damped for 5.5 ms (47,000 turns). The timing of these gymnastics are so arranged that the positrons enter their ring to replace the bunch that was extracted on the previous cycle. Having a larger transverse phase space to be damped, the positrons will remain in their ring twice as long (11 ms). At the start of the next cycle the alternate fully damped bunch is used.

In order to keep all these operations in synchronism, the RF frequencies of the linac, damping rings and subharmonic buncher run at multiples of each other and are phase locked together. Sector 1 of the linac fires 13 microseconds after the main linac in order to give the positrons time to return from source to reinjection point.

The Electron Sources

The SLC can be fed from either thermionic or laser driven photoemission guns each of which is mounted 38 degrees off the axis of the accelerator. The specifications of these devices are listed in Tables 2 and 3. They are followed by two subharmonic velocity modulator cavities at 178.5 MHz, an S band buncher and an accelerator that boosts to 200 MeV. Photo 1 shows both guns in place. The laser gun has been operated in the laboratory producing the required current with the expected 50% polarization. In order to transmit and accelerate electrons and positrons (which have larger emittance, $\gamma\epsilon = 1000 \times 10^{-5}$ m-rad) the first sector of the linac has been equipped with 80 quadrupoles to provide the very strong focusing needed to overcome the effects of transverse wakefields (Photo 2). The system has been in operation in various forms for several years. Thermionically produced pairs of electron bunches have been accelerated to full energy with bunch populations each of 6×10^{10} within the specified emittance and energy spread ($\pm1\%$).

Photo 1. Off-Axis Themionic and Laser e^- Guns.

Table 3: Laser Gun Specifications	
Electrons per pulse	1×10^{11}
Charge per pulse	16 n Coulomb
Repetition rate	180 Hz
Cathode voltage	200 kV
Focusing electrode voltage	125 kV
Anode	Ground potential
Gun insulation	Atmospheric pressure SF_6
Electron pulse width	Varialbe between 80 and 1500 ps
Cathode area (diameter)	1.77 cm^2 (1.5 cm)
Laser mode locking frequency	59.4 MHz
Interpulse spacing	8.40 ns
Electron pulse time stability w.r.t. RF zero crossing	Better than 10 ps
Photocathode material	GaAs
Cathode current	Space charge limited to 15 A peak from 1 cm^2
Pulse to pulse amplitude stability	Better than 5%
Electron polarization	Zero initially, 50% with addition of dye, ~ 100% with $CdSiAs_2$ cathode.
Optical wavelength	1.06 μm from laser, frequency doubled to .532 μm.
Calculated invariant emittance area	$1 \times 10^{-3}\pi m_o c$ cm

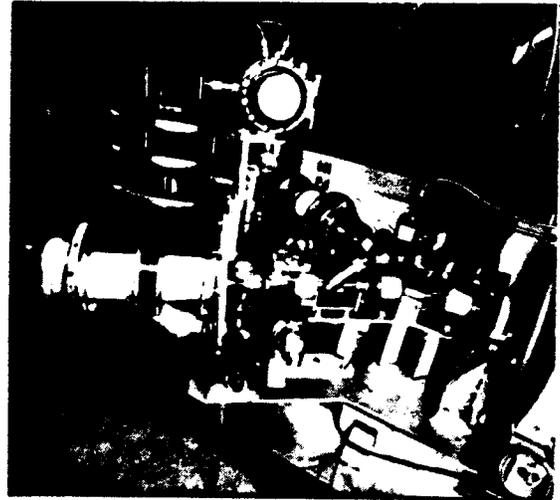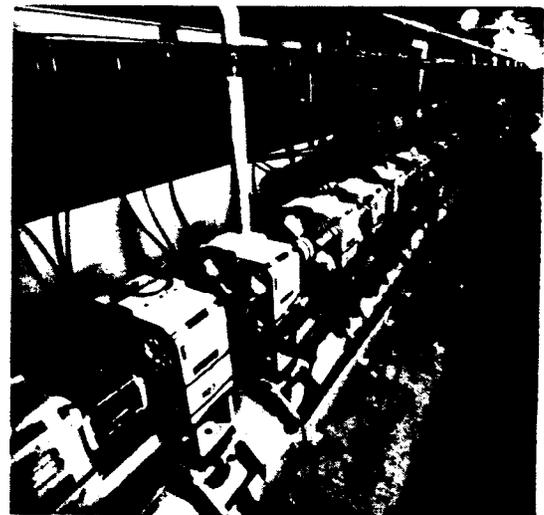| Table 2: Thermionic Gun Specifications	
Type	Triode with intercepting mesh control grid
Electrons per Pulse	1×10^{11}
Charge per Pulse	16 n Coulomb
Pulse Width	2.5 ns FWHM
Repetition Rate	360 Hz
Minimum Interpulse Spacing	8 ns
Cathode Voltage	$\geq$ 150 kV
Anode Voltage	Ground potential
Cathode Area	2 cm^2
Cathode-to-Grid-Spacing	150 μm
Grid Pulse Height	500 V
Pulse-to-Pulse Amplitude Stability	1 %
Calculated Invariant Emittance Area	$3 \times 10^{-3}\pi m_o c$ cm

Photo 2. Strong Focussing on Linac Sector 1.

2

The Damping Ring Complex

Even before SLC project authorization, an electron damping ring was constructed in two years as an R&D vehicle to demonstrate the feasibility of producing beam emittances sufficiently small for linear colliders. First operational in the spring of 1983 it has been a valuable tool to confirm parameter choices and to indicate areas of improvement in component design and fabrication before construction began on the second ring. To date it has stored single bunches of 4×10^{10} electrons and two bunches of 2×10^{10} each. No unexpected storage ring phenomena have been encountered but several significant changes were called for.

1. In the original concept it was planned that both rings be housed in the same vault, one ring mounted above the other. The actual complexity of these compact rings made it evident that both installation of the second ring and serviceability of both rings would be improved sufficiently to justify the cost of separate housings. The geometry of the north complex is shown in Figure 2.
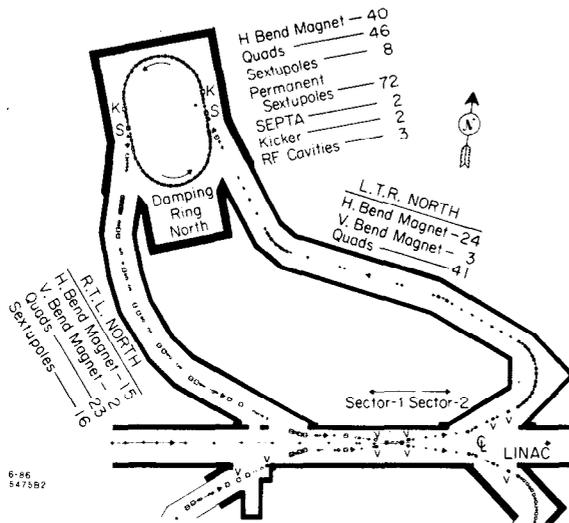

Figure 2. Layout of North Damping Ring Complex.

2. One may note that the shape of the linac to ring transport line (LTR) was predicated by the desire to manipulate the electron's spin polarization vector from longitudinal to upright so that it would not be affected in the ring. The return line (RTL) contains the longitudinal phase compressor which exchanges bunch length for energy spread which in turn calls for achromatic, non-isochronous optics. When the north vault was constructed, the four out and in beam matchings had to be redesigned and rebuilt.

3. Sextupoles had been originally built into the bending magnets by shaping the ends of the poles. Since the dipoles are operated at 2 Tesla, these ends saturated lowering the value of $\int B^2 \cdot d\ell$. Since this term appears in the synchrotron radiation integrals, the expected damping rate was compromised by about 10%. In the new design, the ends of the magnets have been squared, restoring the damping rate and somewhat stronger chromaticity correcting sextupoles were sandwiched in the remaining 2 cm space by employing a compact and efficient rare-earth (SmCo) permanent magnet design.

4. Various other improvements were incorporated. More beam position monitors of a more rugged design were added. The cooling channels of the septa were improved.

5. The horizontal tunes of the rings have been raised by one integer.

The current, slightly revised, parameter list of the rings is shown in Table 4. The new north ring became quickly operational in February of this year and is shown together with its staff in Photo 3. Further testing of this ring was then interrupted because the laboratories' ongoing physics program was interleaved until July. The upgraded south ring is scheduled for tests with electrons in August and September and positron tests in October.

Table 4: Current Design Parameters for Damping Rings		
Energy	1.210	GeV
Circumference	35.270	m
Revolution Frequency	8.50	MHz
RF Frequency	714.000	MHz
Harmonic Number	84	
Transverse Damping Time	3.36	msec
Equilibrium Emittance		
(with full coupling)	6.8×10^{-9}	π rad m
Equilibrium Rel. Energy Spread	7.3×10^{-4}	
Momentum Comp. Factor	.01469	
Energy Loss/Turn	93.1	keV
Bending Radius	2.0372	m
Bending Field	19.812	k gauss
CELL-Structure	1/2 FODO 1/2 F	
ν_x	~ 8.17	variable
ν_y	~ 3.17	variable
Acceptance		
– in Phase Space	$\geq 4.13 \times 10^{-6}$	π rad m
– in Energy	$\geq \pm 1\%$	
RF System and Related Parameter		
– RF-Voltage	800	kV
– Phase	$6.7°$	
– Synchrotron Frequency	107.3	kHz
– Tune	.0126	
– Equilibrium Bunch Length	5.9	mm
$\varepsilon_c =$	1.9283	keV
I (2 bunches)	136.2	ma
P (synchrotron rad)	12.68	kW

Photo 3. North Damping Ring.

The Linac Upgrade

It was recognized at the outset that wakefield considerations would dominate the behavior of intense single bunches passing through the SLC linac. If the bunches are too short longitudinal wakes decelerate the trailing particles causing unwanted energy spread; if the bunches are too long transverse wakes deflect the particles following the head of the bunch causing emittance dilution. A compromise length must be chosen. The former effect is then compensated by placing the bunch ahead of the crest of the RF wave (at the expense of accelerating gradient), the latter effect is controlled by making a precise trajectory correction for the beams so that they pass very close to the center of the RF structure. This requirement imposes stringent tolerances not only on the placement of components in the linac (≈ 100 microns) but also on launch stability at injection, which in turn limits pulse to pulse jitter amplitude in the extraction kickers of the damping rings to $\approx 0.01\%$.

The linac has now been equipped with steering coils and quadrupole-beam-position-monitor packages every 40 foot as shown in Figure 3. for trajectory control of either sign particle. A detailed examination of certain pieces of the original linac accelerating structure showed small constructional asymmetries which would be harmful for SLC type beams. New pieces, screened for this effect, have been inserted.
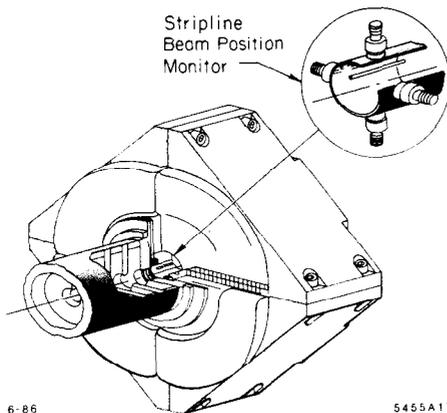

Figure 3. Linac Quadrupole-BPM Package.

When it was realized that bunches traveling down the collider arcs would emerge shorter than when they entered (due to a pathlength-energy correlation) thereby reducing the desirable pinch effect, it was decided to inject into the linac with a length of 1.5 rather than 1 mm. To combat the resulting transverse effects, the focusing in sectors 2, 3 and 4 was increased. This was accomplished by shortening a number of standard 10 foot waveguides by 6 inches and inserting quadrupoles. The resulting strong focusing lattice is shown in Figure 4.

Computer simulations of Landau damping (up to $\Delta E/E \approx 5\%$ at sector 4) have shown the efficacy of the method, providing a reduction of a factor of about 10 in sensitivity to steering errors.[4] New instrumentation required for emittance, energy, energy spread monitoring and control have been developed.
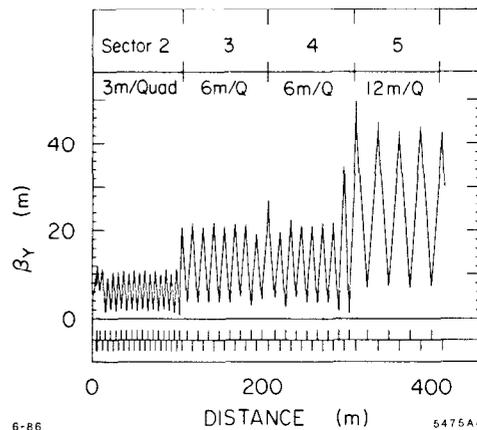

Figure 4. Quad Lattice in Linac Sectors 2-5.

The energy spread monitor[5] consists of a vertical magnetic chicane, placed in the linac to arc region at a point having considerable horizontal dispersion, from which synchrotron radiation x-rays will be detected on a pulse by pulse basis.

Linac performance: As early ago as February 1984, a single bunch intensity of 1×10^{10} electrons/bunch was observed within an invariant phase space of $\gamma \epsilon_{x,y} = 4 \times 10^{-5}$ m-rad at sector 10, a location 1/3 of the linac's length. This measurement was consistent with design specification. Since then the rest of the linac underwent the upgrading process. Tests to the end of the linac will resume on August 25th.

Klystron and Modulator Upgrade[6]

In order to reach an energy of 50 GeV at the collision point and allow for beam loading, off crest operation, energy loss in the arcs, provision for Landau damping and the like, the linac will be run in SLED II mode with new higher power S-Band klystrons operating with a longer pulse. The SLED II waveform is shown in Figure 5.
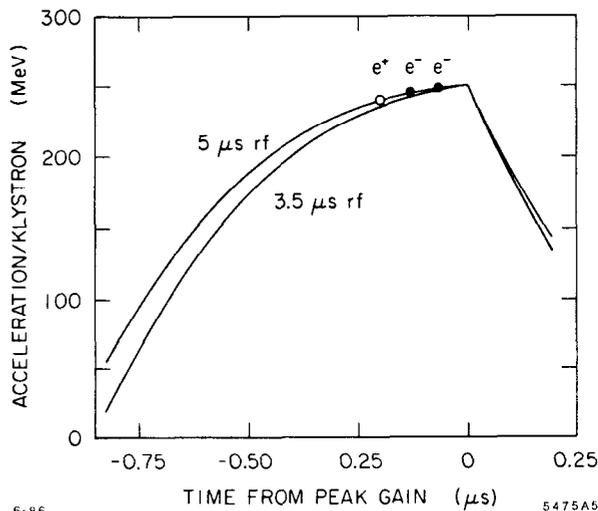

Figure 5. Energy Gain of SLED II Waveform.

Sectors 2-30 (2900 meters) will be powered by 229 nominally 50 MW tubes of SLAC design and manufacture. Such tubes is shown in Photo 4; their nominal specifications are listed in column 2 of Table 5. The problem of extracting power through the ceramic output window has been solved by the use of two windows in parallel. It has been found that these tubes operate better at 60 to 70 MW with a shorter pulse (3.6 usec). The revised operating parameters are shown in column 3 of Table 5. To date there are about 165 of these tubes in service on the linac. They are currently manufactured at the rate of 11 starts/month with a yield of between 70% to 80%. This high yield is the result of extensive quality control measures. Waveguide vacuum valves are being replaced to handle the higher power.

Modulators are being rebuilt to the new specifications (350 kV and 450 amperes). The new system will be run initially at 120 Hz rather than 180 Hz to keep the average power within the existing modulator's transformer capability. This reduction accounts for one of the terms in the aforementioned "initial" luminosity goal. Future modifications to the modulator will restore operation at 180 Hz.
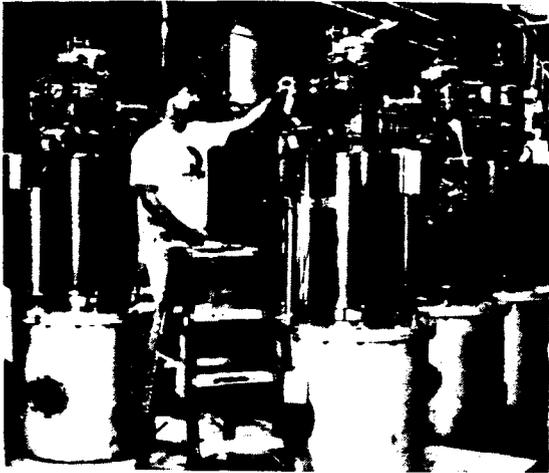

Photo 4. New Klystrons with Their Oil Tanks.

Table 5: Klystron-Modulator Specifications		
	Nominal	Actual
Klystron Peak Output Power	50 MW	67 MW
Frequency	2856 MHz	2856 MHz
Perveance	2×10^{-6}	2×10^{-6}
Peak Beam Voltage	315 kV	350 kV
Peak Beam Current	354 A	414 A
Peak Beam Power	111.5 MW	145 MW
Average Beam Power	120.3 kW	117.5 kW at 180
Klystron Impedance	890 Ω	850 Ω
RF Pulse Width	5 μsec	3.5 μsec
Modulator Pulse Width	6 μsec	4.5 μsec
Repetition Rate	180 pps	180 pps
Klystron Efficiency	0.45	0.46
Pulse Transformer Ratio	1:14	1:15
PFN Impedance	4.6 Ω	3.9 Ω
dc Power	141.6 kW	95 kW at 120
ac Power	157.5 kVA	105 at 120
Focusing Magnet	Electromagnet	Electromagnet
Cathode Type	Dispenser	Dispenser

The Positron Source

The positron source system is shown schematically in Figure 6 and its specifications are listed in Table 6. Of particular interest is the rotary pair production target and solenoidal collector package. It is shown in Figure 7.
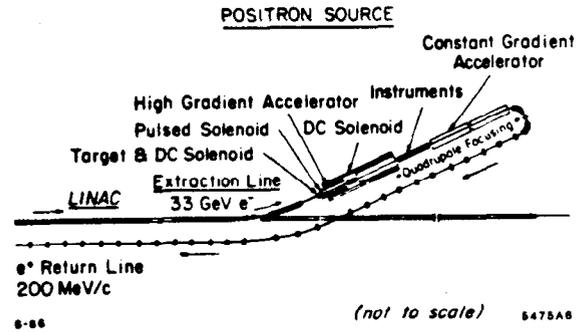

Figure 6. Schematic of the Positron Source.

| Table 6: Positron Source Specifications	
Electron Scavenger Pulse	
Energy	33 GeV
Intensity	5.0×10^{10} e^+/pulse
Size (1σ)	0.6 mm
Pulse Energy	264 Joules
Pulse Rate	180 Hz
Power	47 kW
Target	
Material	90% Ta – 10% W
Energy Deposition	53 J/pulse
Pulse Temperature Rise	380° C
Max. Compressive Stress	32,000 psi
Length	$6 X_o = 24$ mm
Power Deposition	9 kW
Max. Pulse Temp.	580°C
Steady-State Temp.	200°C
Positron Beam at Target	
Energy Range	2-20 MeV
Transverse Emittance	2 mm × 2.5 MeV/c
Invariant Transverse Emittance	0.01 m
Yield (e^+/e^- in.)	2.5
Beam at End of Sector 1	
Energy	1.21 GeV
Energy Spread	2% full
Transverse Emittance	4.2×10^{-6} m rad
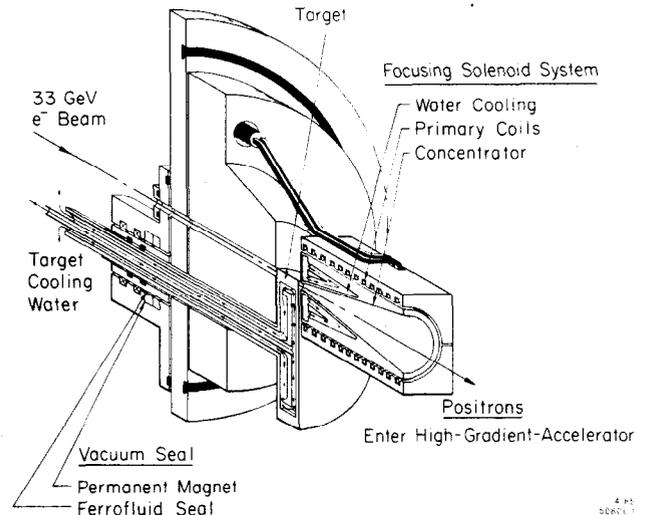
Figure 7. Positron Target and Focusing Horn.

Extensive tests on the tantalum-10% tungsten target material have shown that it should survive provided the incoming beam particle density does not exceed $10^{11}/\text{mm}^2$. This translates to beam dimensions of $\geq \sigma = 600\ \mu$.

The collector solenoid also has some interesting parameters. The 14 turn primary has run (in air) at 7.6 kV, 10.5 kA, 120 pps producing a peak field of 8 Tesla in the throat of the flux concentrator (exceeding design values with a substantial margin).

The 1.5 m high gradient accelerator[7] which immediately follows the collector is powered to produce a beam loaded gradient of 55 MeV/m and is followed by 3 standard 10 foot acceleration sections to boost the positrons to 200 MeV. Solenoidal focusing is provided on the first two sections, strong wraparound quadrupole focusing on the last two. The beam is then sent through an isochronous vertical 180° turn around and returned to the head of the linac via a FODO array 2 km long with quadrupole, beam position monitor and steering packages every 12.7 meters.

The whole system was completed in May. In July, electrons were extracted via the channel shown in Photo 5, targeted on the converter and positrons were accelerated. Tests continue this month. Note a portion of the positron return line which can be seen mounted from the tunnel ceiling.

Photo 5. 33 GeV e^- Extraction Line, e^+ Return Line.

The Collider Arcs

The purpose of the Arc transport system is to bend the electron and positron beams from the linac around to allow head-on collisions. This must be accomplished with a minimum of phase space dilution and energy loss. To combat emittance growth due to quantum effects in the synchrotron radiation process, the adopted design utilizes an alternate gradient transport with large radius of curvature, $\approx 95\%$ circumference factor, and very high gradient to suppress the dispersion function. The betatron phase advance is 108 degrees per FD cell, 10 cells comprise an achromat and each ≈ 1 km long arm contains a train of 23 achromats. These achromatic optics provide a momentum pass band of $\pm 0.5\%$. The planes of individual achromats are rolled about the local beam axis so that the trajectory follows the topology of the site's terrain. The tunnels, which dip as much as 30 meters near mid-point, contain grades up to 10%.
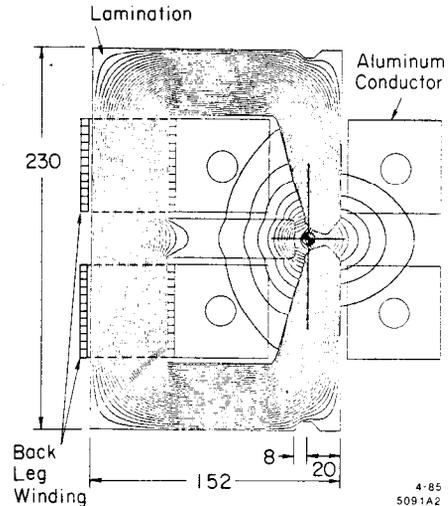

Figure 8. Cross Section of Alternate Gradient Magnet.

Each AG magnet is 2.5 m long and has a cross section shown schematically in Figure 8. At 50 GeV the guide field is 5.98 kG on which a gradient of ± 7.02 kG/cm and a sextupolar term $\approx \pm 2$ kG/cm^2 have been superimposed. Extensive computer simulated error analyses[8] have shown that the expected magnet to magnet alignment of these strong quadrupoles (even as small as $\approx 100\ \mu$rms), will be insufficient to maintain the desired optical characteristics of the system. It was therefore decided that each of the over 900 magnets be provided with a motor activated positioning mechanism and a high resolution beam position monitor so that the beam itself can be used for centroid correction of the orbit.

Photo 6 shows a portion of the south tunnel. All the magnets in a given arc are excited in series by current bars threaded through them. Backleg windings are used to correct the field strengths along the arcs for synchrotron radiation energy loss which, at an input energy of 51.4 GeV, amounts to 1.4 GeV.
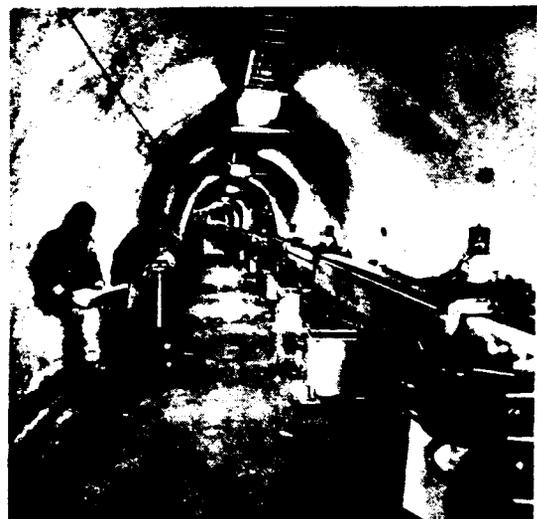

Photo 6. Portion of Arc Tunnel with AG Magnets.

All the magnets have now been built, measured, fitted with their 1.2 cm diameter vacuum chambers and installed with bus bars in their preassigned locations in the ring. All beam position monitors, which span the AG magnets, have been calibrated and are being installed. All magnetic components of the special beam matching sections are mounted. It remains to complete the high power input momentum defining slits, certain beam emittance and diagnostic instruments, the beam protection system and, most importantly, computer checkout of hardware and software. The system is scheduled for beam tests mid October.

The Final Focus

The final focus system, filling the last 152 meters of tunnel on either side of the interaction point, contains the elements that demagnify the beams to a final spot size of about 2 μm, steer them into collision, and transport the disrupted outgoing beams to 70 kW absorbers. The optics design utilizes telescopic modules with simultaneous point to point and parallel to parallel focusing to minimize the magnitude of higher order optical distortions. A chromatic correction module is incorporated to handle a finite input momentum spread up to $\pm 0.5\%$ The final focussing triplet packages, the last elements of which presently reside 2.8 meters from the I.P. need to be as strong as feasible. Optical and hardware designs exist for both superconducting and normal quadrupoles. Initial operation will be with conventional magnets to alleviate worries of beam induced quenches. This decision results in a 20% reduction of initial luminosity but will be made up when the superconducting lenses (already being built and successfully tested at FNAL) are employed. There are some 160 magnetic elements in this system one half of which is shown schematically in Figure 9. Figure 10 shows how the triplet and the Mark II detector fit with respect to each other. To gain access to the central drift chamber, the barrel containing the triplet is rolled back on precision rails so that the magnet door and endcap calorimeter can be retracted.
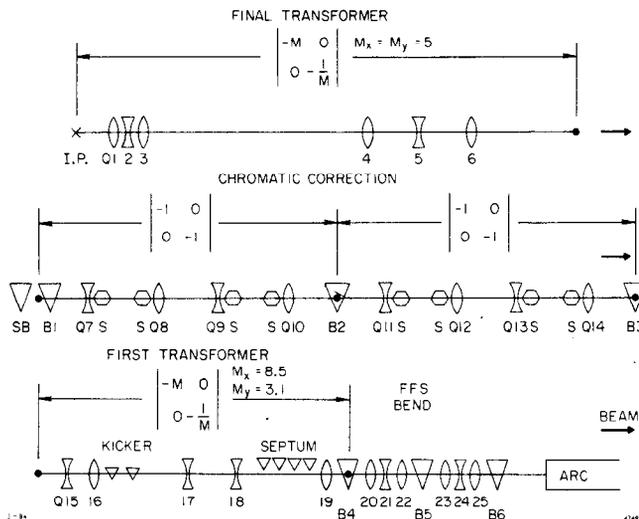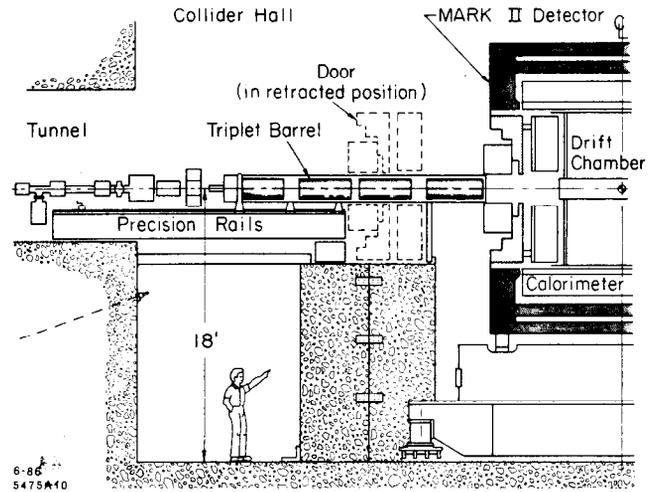
Figure 10. Final Triplet in Relation to Mark II.

A question often asked is: "How does one steer micron sized beams, that emanate from essentially separate transport systems, into collision?" The planned steps are as follows: (1) After very careful mechanical alignment, single beams are sent across the I.P. with the final triplets turned off and observed on high resolution (10 micron) beam position monitors. The final lenses are then turned on and their mechanical position adjusted by special cam driven movers to re-center the beams. (2) The relative position of two beams can then be measured in a single monitor whose directional strip line properties permit distinguishing one beam from the other. (3) If the beams pass each other with an offset of ≤ 50 μ they will deflect each other through angles[9] that are measurable by turning off one or the other beam. The magnitude and phase of this effect, for some given set of parameters, is shown in Figure 11. Wire scanners, containing 7 μ carbon fibers, are being constructed for low current adjustment of beam size. In full current operation, the flux and spectrum of the beamstrahlung[10] effect, and/or the magnitude of beam-beam disruption angles can be monitored to adjust for peak luminosity.

This system of the SLC, being the last to receive beams, has been the last to reach fabrication stage. At this time most of the magnets and other components are finished and are awaiting either final calibration or mounting on their support girders. Beam tests are scheduled for the end of December.
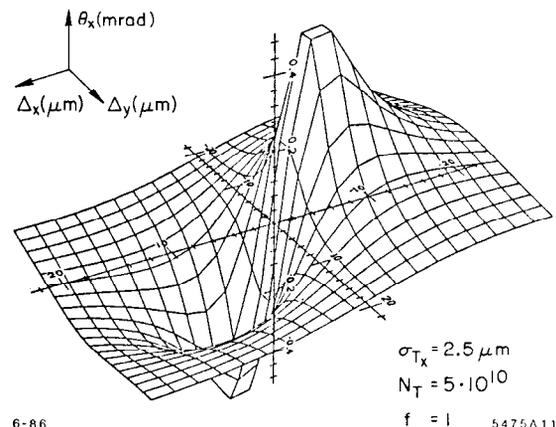
Figure 9. Schematic of FFS Optical Layout.

Figure 11. Horizontal Beam-Beam Deflection vs. Δ_x, Δ_y

The Control System

An entirely new control system was developed for all SLC systems. It consists of two central processors (VAX 780) with distributed intelligence in the form of multibus microcomputers which in turn control CAMAC crates. Communication throughout the net is via a broad-band 3/4″ CATV coax cable with a data rate of 1 Megabaud. Operator interface is by means of consoles on wheels (COW) that can be connected anywhere on site. The system is designed to control SLC via optics driven models which are standardized, as much as is feasible, with respect to interface and software. One of the new features is the control, monitoring and stabilization of all klystron amplitudes and phases in the linac. This will improve the ease with which beams are set up and maintained by operators. An elaborate timing system with programmable delay units is operational. Although the system has been in operation since January of 1984 a recent addition is notable. It consists of two "work stations" (DEC VAXstation II/GPX) each possessing about 80% of the computational power of a VAX and which contain extensive graphics and "window" capabilities with the aim of improving machine-operator communication. The screen of one of these mouse driven work stations is shown in Photo 7. Applications software development continues.
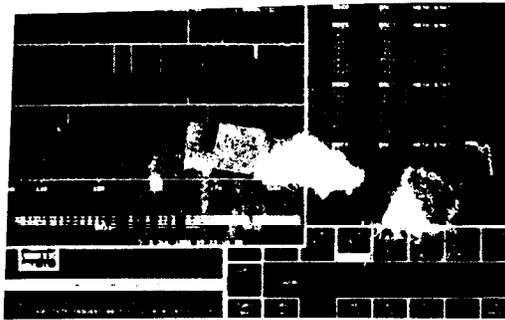

Photo 7. Workstation Screen with "Window" Displays.

Conventional Construction

The north damping ring vault was completed December 1984, the arc tunnels in May 1985. Photo 8 is an early aerial view of the SLAC site showing the only manifestation of the SLC that is visible from above – the excavation of the Collider Experimental Hall (CEH). The building was completed June 1986 and is divided into three regions by the use of removable concrete block shielding walls.

Photo 8. SLAC Site Showing CEH Excavation.

The central (IP) region is 16 by 19 meters and is flanked by two assembly bays of 23 by 19 and 32 by 19 meters in order to house the two detectors in a push-pull arrangement. Photo 9 shows the central 400 ton portion of the venerable but improved Mark II detector, which had seen service at both SPEAR and PEP being lowered into the pit for physics next spring.
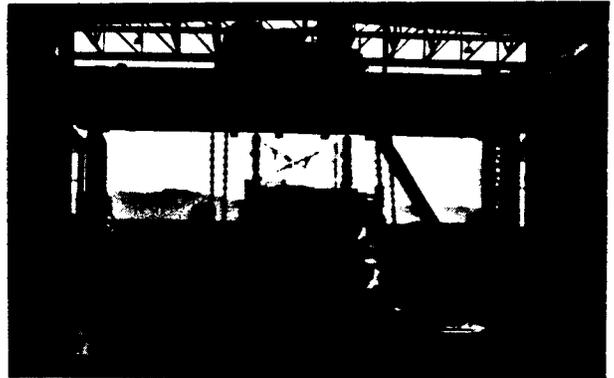

Photo 9. Mark II Detector About to be Lowered into Pit.

References

1. B. Richter, 11th International Conference on High Energy Accelerators, Geneva, 1980, p. 168.

2. SLC Design Handbook, Stanford Linear Accelerator Center, December 1984.

3. S.D. Ecklund, "The Status of SLC," IEEE Trans. Nucl. Sci. NS-5, 1592, October 1985.

4. J.T. Seeman and J.C. Sheppard, "Special SLC Linac Developments," SLAC-PUB-3944, May 1986.

5. J. Seeman, W. Brunk, M. Ross, E. Tilleman and D.Walz, "SLC Energy Spectrum Monitor Using Synchrotron Radiation," SLAC-PUB-3945, April 1986.

6. M.A. Allen et al., "Operational Experience with SLAC Energy Upgrade," SLAC-PUB-3941, April 1986.

7. H.A. Hoag, H. Deruyter, J. Kramer and C.G.Yao, "Capture Section for the SLC Positron Source," SLAC-PUB-3971, May 1986.

8. S. Kheifets, T. Fieguth, K.L. Brown, A. Chao, J.J. Murray, R.V. Servranckx and H. Wiedemann, "Beam Optical Design and Studies of the SLC Arcs," SLAC-PUB-4013, June 1986 and these Proceedings.

9. P. Bambade and R. Erickson, "Beam-Beam Deflections as an Interaction Point Diagnostic," SLAC-PUB-3979, May 1986.

10. G. Bonvicini, J. Ferrie, C. Field and A. Minten, "Beamstrahlung Monitor for SLC Final Focus," SLAC-PUB-3978 and SLAC-PUB-3980, May 1986.

11. J. Rees, "A Progress Report on the SLAC Linear Collider," SLAC-PUB-3986, June 1986.